NURETH14-xxx

CFD SIMULATIONS OF A TURBULENT FLOW IN A T-JUNCTION

T. Morii¹, Y. Onishi², K. Hirakawa² and I. Nakamori²

¹ Japan Nuclear Energy Safety Organization, Toranomon, Tokyo, Japan

² AdvanceSoft Akasaka, Tokyo, Japan

Abstract

Very careful T-junction tests are being performed at the Vattenfall Älkarleby Laboratory. Data from a recent test were used as the basis of an OECD/NEA blind benchmark exercise. JNES participated in this blind benchmark exercise. The present T-junction CFD simulation was performed as an incompressible fluid flow and buoyant effect was estimated by using the Boussinesq approximation. Four hexahedral grids (0.25M, 1M, 4M and 16M) were generated for grid size sensitivity study. The Large Eddy Simulation (LES) and the Reynolds Averaged Navier Stokes (RANS) turbulent models were used for a model sensitivity study. All calculation results of LES were closer to the experimental data than those of RANS.

Introduction

The availability of robust commercial CFD software and high speed computing leads to the increasing use of CFD for the solution of fluid engineering problems across all industrial sectors, including the nuclear reactor safety problems. JNES has developed a state-of-the-art CFD capability that supports the Japanese regulatory activities.

Recently, however, there has been growing awareness that CFD methods can prove difficult to apply reliably, i.e. with a known level of accuracy. Verification and Validation (V&V) [1] of CFD results are one of key issues on applying CFD to nuclear reactor safety that needs high reliability of calculated results. Briefly, verification is the assessment or estimation of the numerical accuracy of the solution to a given computational model. Validation is the assessment of the accuracy of a computational model through comparison of computational simulations with experimental data.

Very careful T-junction tests have been performed at the Vattenfall Älkarleby Laboratory in Sweden, and these data are appropriate to the needs of the CFD code validation. Therefore, data from a recent test was used as the basis of an OECD/NEA blind benchmark exercise. JNES participated in this benchmark exercise and submitted the LES simulation results. The present T-junction CFD simulation was performed as an incompressible fluid flow and buoyant effect due to mixing between main cold water (19°C) and T-branch hot water (36°C) was estimated by using the Boussinesq approximation. Size and shape of calculation region, boundary conditions and water properties were specified in the OECD/NEA-Vattenfall T-junction benchmark specifications [2]. Following the OECD/NEA Best Practice Guidelines (BPG) for the use of CFD in nuclear reactor safety applications [3], sensitivities of grid size and turbulent model were studied. Four hexahedral grids (0.25M, 1M, 4M and 16M) were generated for grid size sensitivity study. LES with constant Smagorinsky and RANS turbulent models were used for turbulent model sensitivity study.

1. Analytical method and conditions

1.1 Subheading in a heading section

The CFD code used in these calculations is the Advance/Front/Flow/red code that has been improved by Advance Soft Corporation based on the Japanese open CFD code "Front/Flow/red", which was developed in Frontier Simulation Software by IT program of the Ministry of Education, Culture, Sports, Science and Technology, Japan [4]. The code solved an incompressible fluid flow and buoyant effect due to mixing between main cold water and T-branch hot water was estimated by using the Boussinesq approximation. Since the selection of the turbulent models has crucial influence on CFD simulation results, the calculation results of LES and the RNG k- ϵ model that is a kind of RANS were compared. Calculation of LES required relatively small time steps to reduce numerical diffusion, whereas RANS has been usually applied to steady-state solution.

1.2 Calculation grids

Examination of spatial grid convergence is a sub-task for the verification of the CFD calculation. It is important for the reduction of spatial discretization errors to provide high-quality numerical grid. For mathematically sound grid convergence test, simulations should be carried out on at least three successively refined grids, and the target quantities should be given as a function of the grid width [3]. Following this guidance of BPG, we have made the four successively refined grids (0.25M, 1M, 4M, and 16M). The specific cares in the process of grid generation for T-junction shape shown in Figure 1, that is, width of surface cells become smaller near the junction line of two pipes and faces of inner cells should be vertical to flow direction.

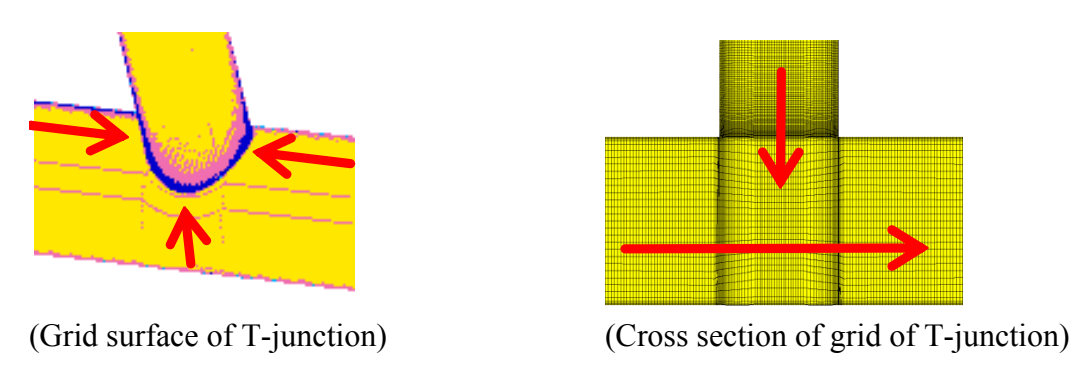


Figure 1 Specific cares in grid generation process.

At last, main characteristics of these hierarchical grids are given in Table.1. Qualities of the grids were carefully maintained for all four grid levels, as documented by the average, the max, and the min. cell sizes and the aspect ratio and skewness of the cells.

		0.25M	1M	4M	16M
Number of cells		230,688	988,800	3,988,708	15,923,386
Average cell	Х	5.239	3.279	2.128	1.264
size	Y	4.619	2.886	1.807	1.254
(mm)	Z	6.616	4.050	2.561	1.809
MAX. cell	Х	9.165	5.744	3.675	2.436
	Y	9.637	6.023	3.853	2.340
size (mm)	Z	21.624	13.519	8.467	2.436
MIN. cell	Х	0.483	0.211	0.131	0.0921
size (mm)	Y	0.491	0.286	0.168	0.0921
	Z	0.509	0.193	0.152	0.101
Aspect ratio	Ave.	4.081	4.174	4.279	3.360
	Max.	27.718	28.579	28.665	16.627
	Min.	1.000	1.000	1.000	1.001
Angle Skewness	Ave.	0.172	0.165	0.168	0.152
	Max.	0.712	0.752	0.715	0.716
	Min.	2.384×10^{-5}	1.047×10^{-5}	3.528×10^{-6}	2.302×10^{-5}
y+		6.4	4	2.6	1.6

Table 1 Main parameters of grid hierarchy

1.3 Analytical conditions

The physical properties of water used in these calculations were provided in the benchmark specification report [2]. In fact, these properties except density were calculated from quadratic and cubic function in the code. The buoyant effect was estimated by using the Boussinesq approximation, where density has been assumed constant and coefficient of volumetric expansion is fitted by the following cubic function.

$$-8.39048 \times 10^{-8} T^{2} + 5.98271 \times 10^{-5} T - 1.01205 \times 10^{-2} \quad T:(K)$$
 (1)

Table 2 shows the boundary conditions used in these calculations. The inlet velocity used in the LES calculation was determined by the auxiliary LES calculation. This type of LES calculations have been performed on the pipe with the periodic boundary condition at both inlet and outlet. Furthermore, the diameter of the pipe has been same as the main and branch pipe respectively, and the length is equal to diameter. As for the turbulent model constant, the effect of the Smagorinsky constant of LES was examined by varying the value from 0.1 (code default value) to 0.2, whereas the turbulent Prandtl number used in LES and RANS were assumed to be 0.9 (code default value).

Table 2 Boundary conditions

		LES	RANS		
Inlet Velocity		the auxiliary LES calculation	experimental data [3]		
	Temperature	rature 19°C (main pipe), 36°C (branch pipe)			
	k and ε	-	experimental data [3]		
Outlet		pressure specified (0Pa)			
Pipe wall	Velocity	Non-slip Attenuation of the Smagorinsky eddy viscosity near the wall	Wall function method		
	Temperature	adiabatic			

Lastly, the conditions of numerical method are summarized in Table 3. Prior to the period for getting the statistical quantities such as average and RMS value, the LES simulation ran for 5 second interval for time-averaged velocities to become statistically steady. After this initial period, five seconds of the transient LES calculation was performed according to the guide of the benchmark specification report [2], whereas, steady state calculation was performed for RANS.

Table 3 Conditions of Numerical Method

		LES	RANS	
Discretized N Equation	Navier-Stokes	Relative Residuals < 10 ⁻⁶ Bicgstab for Matrix solver		
Pressure Equation		Relative Residuals < 10 ⁻⁶ ICCG for Matrix solver		
SIMPLEC	Relaxation factors	Not used	0.3 for pressure equation and 0.8 for other equations	
	Iteration Convergence	Relative Change of variables < 10 ⁻³ , but Maximum Iteration Number equals 3	Relative Change of variables < 10 ⁻⁵	

2. Calculation results

2.1 Metric for comparison between experiment and calculation

The 14th International Topical Meeting on Nuclear Reactor Thermalhydraulics, NURETH-14 Toronto, Ontario, Canada, September 25-30, 2011

Time averaged temperature and temperature fluctuations provided by the organizing committee of the T-junction benchmark were located at 0°, 90°, 180°, and 270°, two, four, six and eight hydraulic diameters downstream of the tee junction, respectively. In addition time dependent temperature readings were provided two and four hydraulic diameters downstream of the tee junction at the four angular locations, at 0°, 180°, and 270° six diameters downstream, and at 0°, 90°, and 180° eight diameters downstream.

PIV data were provided at 1.6, 2.6, 3.6, and 4.6 hydraulic diameters downstream of the tee junction. Time averaged and RMS fluctuations were provided for the x and z velocity components along a vertical line through the center of the pipe at the four x locations. Time averaged and RMS fluctuations were provided for the x and y velocity components along a horizontal line through the center of the pipe at the same four x locations. Figure 2 shows the schematic figure of locations of the provided experimental data.

Following the benchmark specification report [2], a non-dimensional temperature T* and velocity U* was defined for comparison between experiment and calculation. T* is the actual temperature minus the cold flow inlet temperature, divided by the difference between hot and cold inlet temperatures: that is,

$$T^* = \frac{T - T_{cold}}{T_{hot} - T_{cold}} \tag{2}$$

U* is the actual velocity divided by the bulk velocity: that is,

$$U^* = \frac{U}{U_{bulk}} \tag{3}$$

For the present benchmark case, the value $T_{hot}=36^{\circ}C$, $T_{cold}=19^{\circ}C$, and $U_{bulk}=0.975$ m/s are to be used.

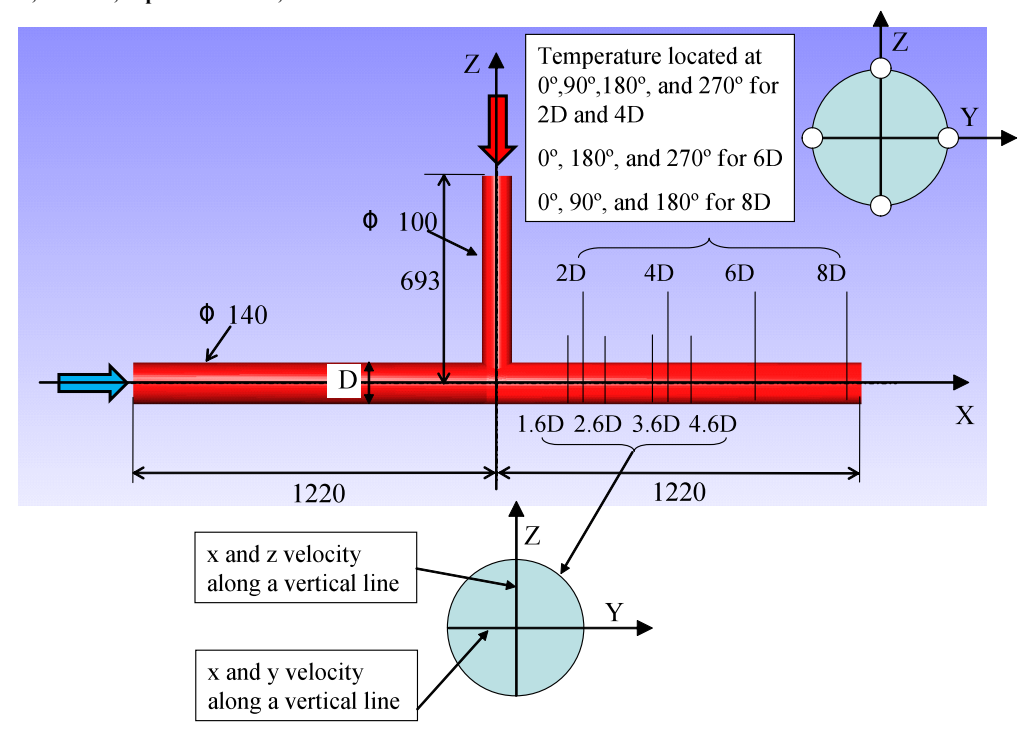


Figure 2 Schematic figure of locations of experimental data.

Among a large number of possible comparison methods between experiment and calculation, a good starting point was needed for the synthesis of results. For any given curve (e.g. x component of time averaged velocity along a vertical line through the pipe center at 2.6 hydraulic diameters downstream of the tee junction) the metric M is defined as:

$$M = \sqrt{\frac{\sum_{i=1}^{N} (C_i - D_i)^2}{N}}$$
 (4)

where N is the total number of comparison points, Ci is the ith results from the CFD calculation and Di is the experimental data at the same location.

These metrics were generated for the LES calculations using all comparisons of time averaged temperatures, RMS temperature fluctuations, time averaged velocity components except y velocity component, and RMS velocity fluctuations. As to this exclusion of y velocity component, we followed the keynote talks for synthesis of T-junction benchmark results [5], i.e., because of the symmetry plane in the experiment, this time average should in theory be zero. However, small unreported asymmetries in the experiment result in non-zero values.

Table 4 shows the summation results of metrics for all calculations. The values in the temperature column of Table 4 mean a sum of the four metrics for temperature (0° at two, four, six and eight hydraulic diameters downstream of the tee junction, 90°, 180°, and 270° at the same diameters downstream respectively). Furthermore, the values in the time averaged velocity column of the table

mean a sum of the twelve metrics (4 metrics for x velocity components along a vertical line through the center of the pipe at 1.6, 2.6, 3.6, and 4.6 hydraulic diameters downstream of the tee junction, 4 metrics for z velocity components along the same vertical line at the same four x locations, and 4 metrics for x velocity components along a horizontal line at the same four x locations). Lastly, the values in the RMS velocity column of the table mean a sum of the sixteen metrics (4 metrics for x velocity components along a vertical line through the center of the pipe at 1.6, 2.6, 3.6, and 4.6 hydraulic diameters downstream of the tee junction, 4 metrics for z velocity components along the same vertical line at the same four x locations, 4 metrics for x velocity components along a horizontal line at the same four x locations, and 4 metrics for y velocity components along the same horizontal line at the same four x locations).

	Number of grids	C_s	Temperature (T*)		Velocity (U*)	
			Time averaged	RMS	Time averaged	RMS
LES	0.25M	0.1	0.3179	0.1114	1.015	0.6748
	1M	0.1	0.3014	0.0928	0.7459	0.6566
	4M	0.1	0.3784	0.1241	0.8650	0.5338
	4M	0.15	0.2542	0.1082	0.7357	0.5929
	16M	0.15	0.3201	0.1189	0.6778	0.5353
	4M	0.2	0.2630	0.1488	0.9855	0.5899
RANS	0.25M		0.6842	-	1.727	
	1M	-	0.6418		1.549	_
	4M		0.6128		1.596	
	16M		0.6479		1.646	

Table 4 Summation of metrics for all calculations

2.2 LES calculations

BPG stated that for mathematically sound grid convergence tests, simulations should be carried out on at least three successively refined grids, and the target quantities should be given as a function of the grid width (or total number of grid points in case of the unstructured grid system). Figure 3 and Figure 4 are drawn for velocity and temperature metrics of the five LES calculations of Cs=0.1 and 0.15 shown in Table 4. It can be seen from Figure 3 that the three calculated velocity fields of LES with Cs=0.1 seems to reach the convergence field around 4M grid points, however, since Cs changes to 0.15, LES solutions start again to approach experimental data as the number of grid points increase and seems not to reach the convergence field. On the other hand, Figure 4 shows that calculated temperature fields of LES do not always approach experimental data as the grid is refined.

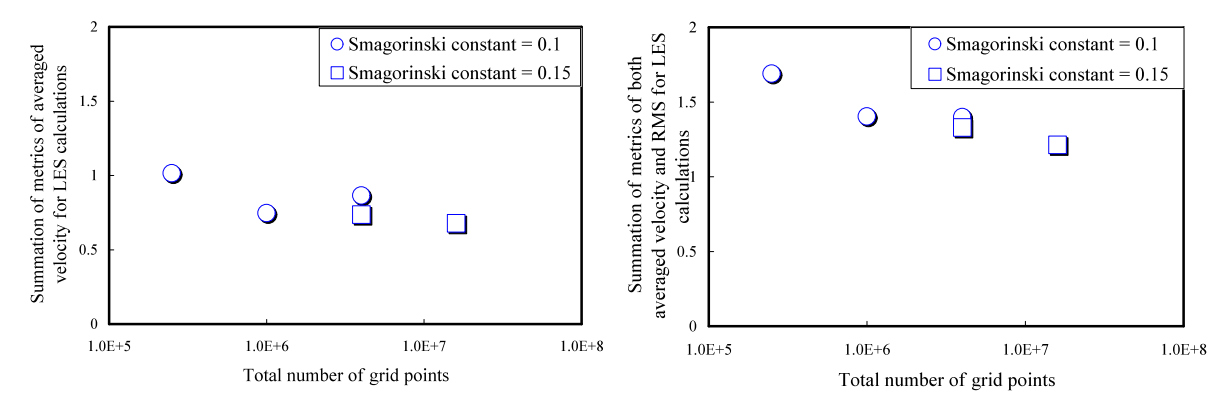


Figure 3 Velocity metrics of LES calculations (dependency for total number of grid points).

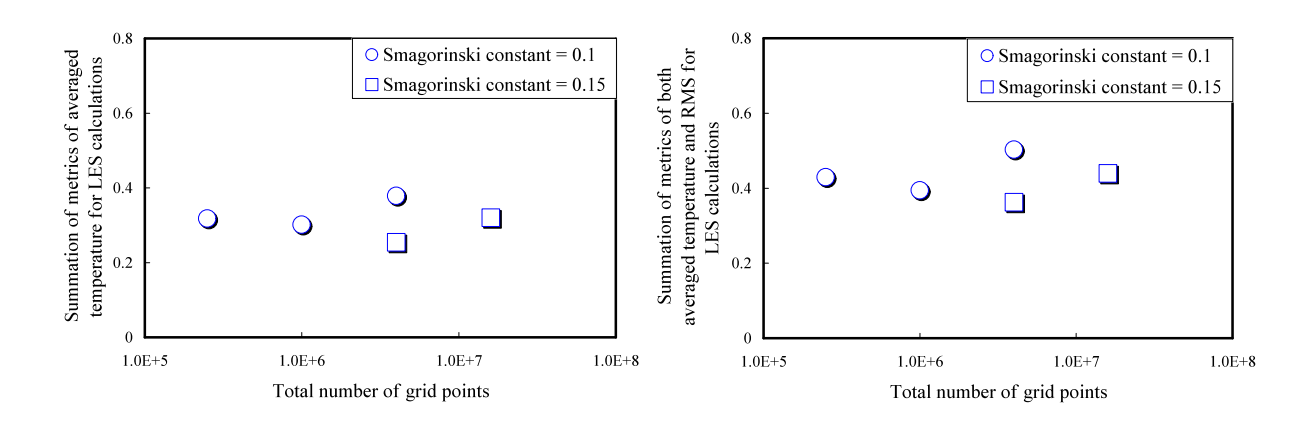


Figure 4 Temperature metrics of LES calculations (dependency for total number of grid points).

2.3 RANS calculations

Figure 5 is drawn for velocity and temperature metrics of the four RANS calculations shown in Table 4. It can be seen from the figure that the calculated velocity and temperature fields of RANS seems to reach convergence around 4M grid points.

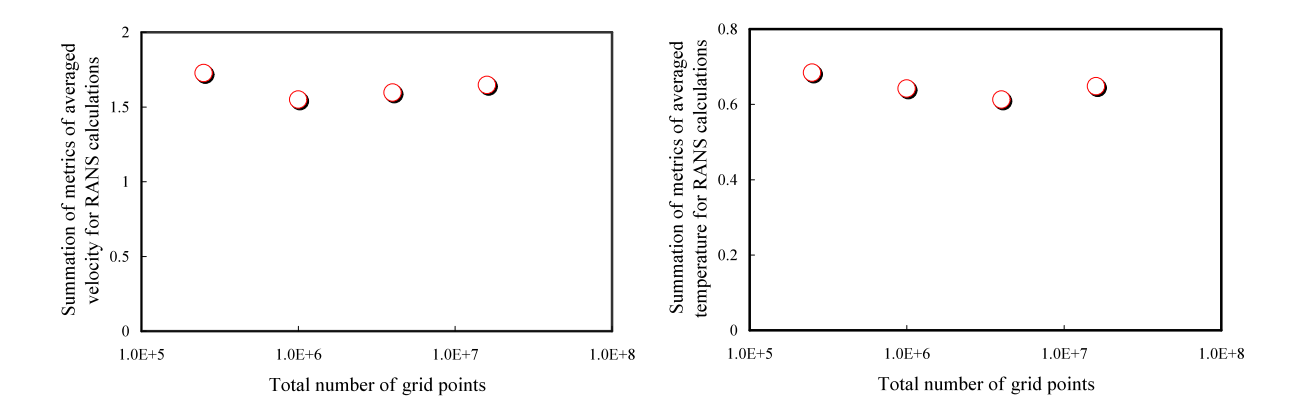


Figure 5 Velocity and temperature metrics of RANS calculations (dependency for total number of grid points).

Figure 6 is a comparison between velocity and temperature metrics of the LES and RANS calculations shown in Table 4. Undoubtedly, the figure shows all calculation results of LES to be closer to the experimental data than those of RANS.

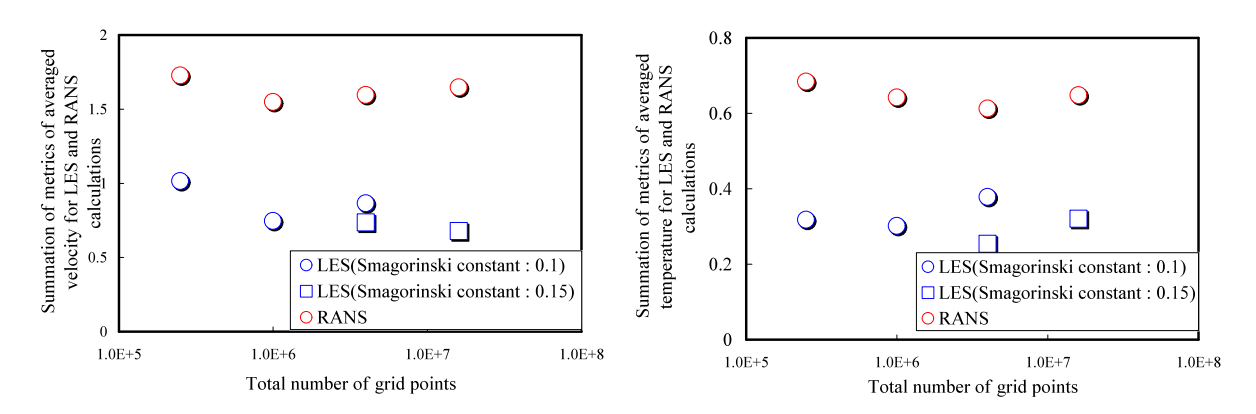


Figure 6 Comparison between metrics of LES and RANS calculations.

2.4 Discussion

Figure 7 shows comparison between the calculated averaged temperature of LES and RANS of 16M grid points with experimental data. Figure 8 shows the colour contours of the calculated averaged temperature of LES and RANS.

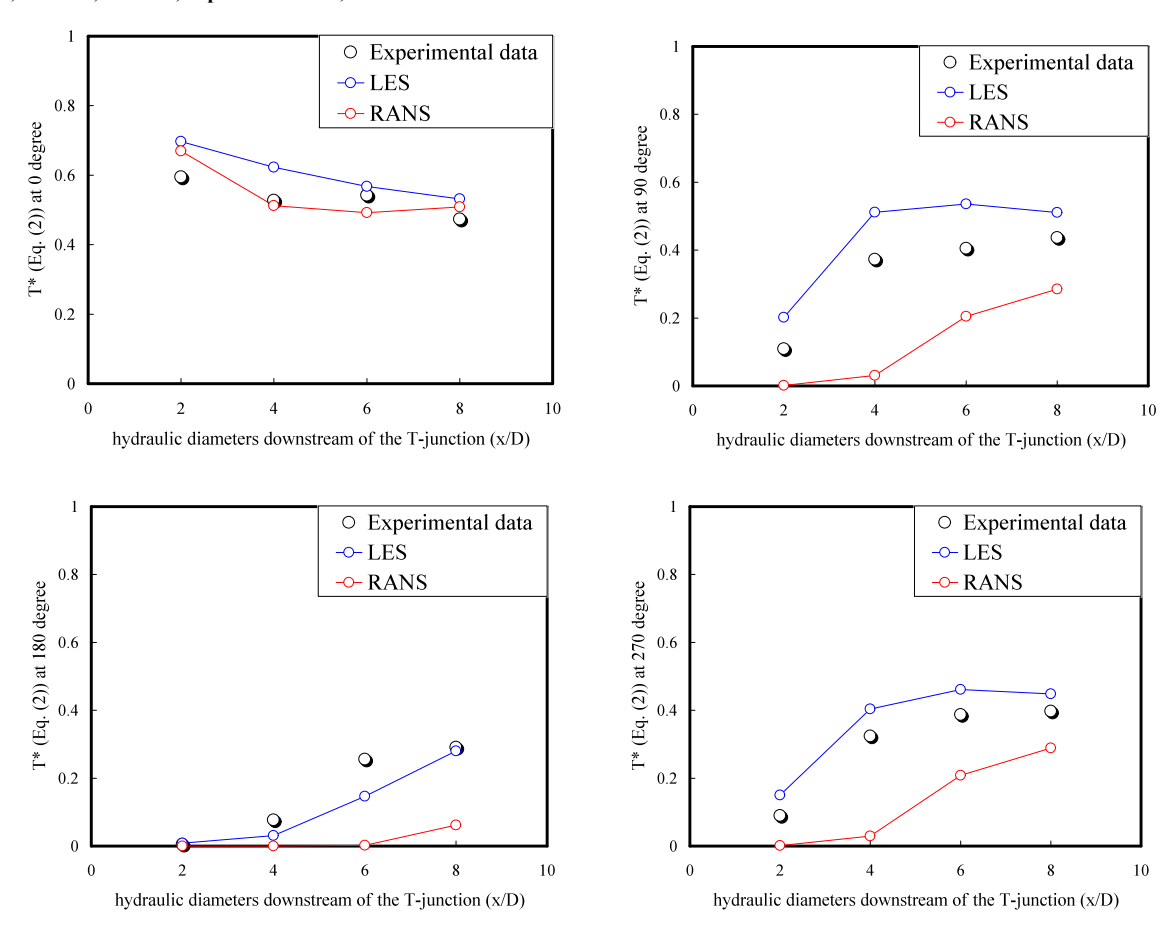


Figure 7 Comparison of averaged temperature of experimental data, LES and RANS at 0°, 90°, 180°, and 270° of main pipe.

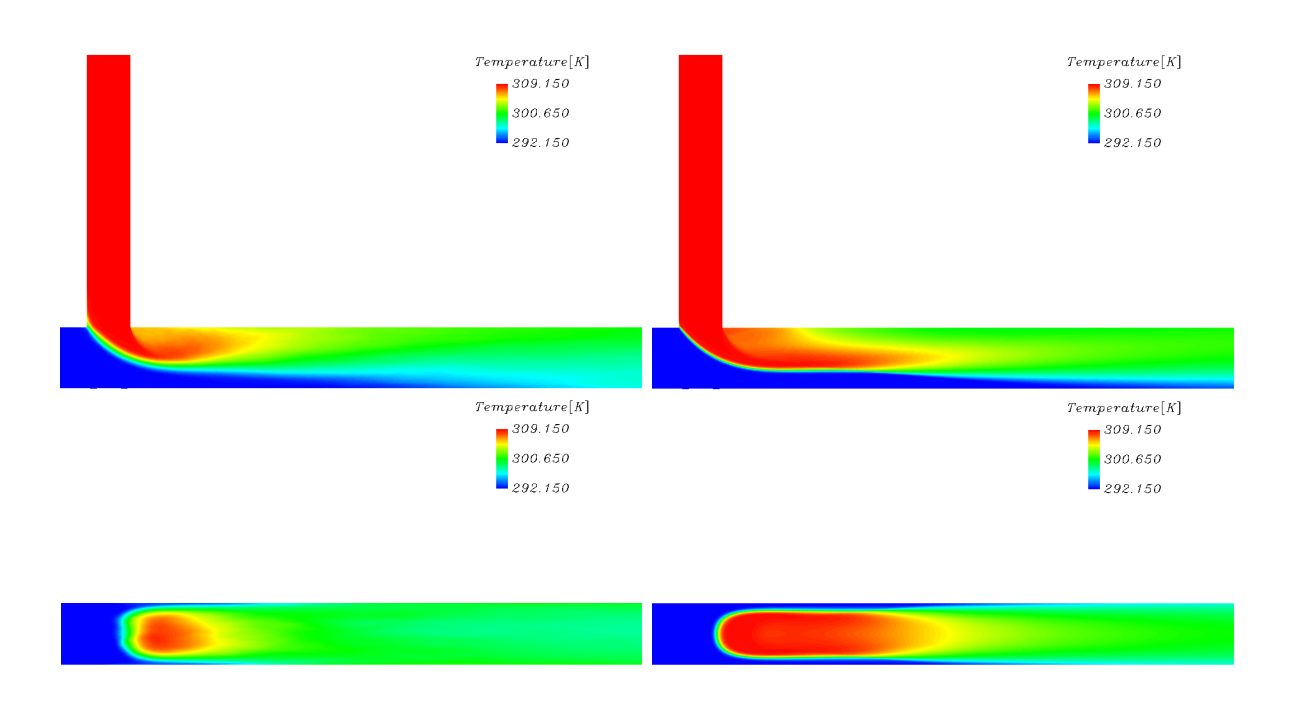


Figure 8 Comparison of averaged temperature of experimental data, LES and RANS at 0°, 90°, 180°, and 270° of main pipe.

Hot water of the branch pipe does not mix with the cold water immediately in the T-junction, but concentrate in the center and the upper part of the main pipe, while cold water of the main pipe flows around the hot water. Meanwhile, turbulence begins to mix hot and cold water together more than 2.0 hydraulic diameters downstream of the T-junction (see Figure 8 and 9). Because RANS underestimate turbulent mixing, calculation results shows that hot and cold water begin to mix around five hydraulic diameters downstream of the T-junction. On the other hand, LES calculations reproduce the experimental results rather well.

3. Conclusions

Among a large number of possible comparison methods between experiment and calculation, a good starting point was needed for the synthesis of results. The present study used rather simple metrics in the manner of the keynote talks for synthesis of T-junction benchmark results [5]. The calculated velocity fields of LES with Cs=0.1 seems to reach the convergence field around 4M grid points, however, since Cs changes to 0.15, LES solutions start again to approach experimental data as the number of grid points increase. On the other hand, the calculated temperature fields of LES do not always approach experimental data as the grid is refined. Though the calculated velocity and temperature fields of RANS seems to reach the convergence field around 4M grid points, all calculation results of RANS are farther away from the experimental data than those of LES.

Acknowledgments

This work was sponsored by the Ministry of Economy, Trade and Industry.

The 14th International Topical Meeting on Nuclear Reactor Thermalhydraulics, NURETH-14 Toronto, Ontario, Canada, September 25-30, 2011

4. References

- [1] W.L.Oberkampf and T.G. Trucano, "Verification and Validation in Computational Fluid Dynamics," SANDIA report, SAND2002-0529, March (2002).
- [2] OECD/NEA-VATTENFALL, "T-junction Benchmark Specifications (Final Version)", July 2009.
- [3] Mahaffey J. et al., 2007, "Best Practice Guidelines for the Use of CFD in Nuclear Reactor Safety Applications", NES/CSNI/R (2007).
- [4] http://www.ciss.iis.u-tokyo.ac.jp/english/dl/index.php (2007).
- [5] J.Mahaffy, "Synthesis of results for the tee-junction benchmark," keynote talks in CFD for Nuclear Reactor Safety Applications (CFD4NRS-3) Workshop, Bethesda, MD, (2010).